rations are strongly linked to many late pathological changes.

Low dose rate irradiation of human populations will be produced by internally deposited radioactive materials acquired from the environment. When data obtained from experimental animals are used to estimate human risk, it is beneficial to have low LET reference irradiation delivered at both high and low dose rates. Utilizing a slowly dividing cell system, such as the liver, and recording chromosome damage after a variety of exposure types may have a very real relationship to genetic risk from protracted radiation exposures.

Genetic hazards are currently estimated for high LET radiation by using brief low LET exposures as a reference. Under these conditions, RBE increases as dose and dose rate decrease. The ICRP (*13*) has thus speculated that if protracted low LET radiation has been used as a reference standard for genetic damage, it may be necessary to substantially increase the quality factors now used for protection of the human population from genetic effects of high LET irradiation. The results reported here illustrate that this is not the case. The RBE of alpha emitters, when compared with protracted exposures to beta or gamma emitters, ranges from 15 to 20 even when very low dose rates of beta and gamma are used as a reference irradiation. The quality factor of 10 used by the NCRP and ICRP to estimate risk from high LET irradiation may be low by as much as a factor of 2, but no gross reevaluation seems needed.

ANTONE L. BROOKS
Inhalation Toxicology Research Institute, Lovelace Foundation, Albuquerque, New Mexico 87115

References and Notes

1. *Basic Radiation Protection Criteria* (NCRP No. 39, National Council on Radiation Protection and Measurements, Washington, D.C., 1971), p. 28.
2. A. L. Brooks, R. F. Peters, M. D. Rollag, *Radiat. Res.* **45**, 191 (1971).
3. A. L. Brooks, D. K. Mead, R. F. Peters, *Int. J. Radiat. Biol.* **20**, 599 (1971).
4. K. Sax, *Genetics* **23**, 494 (1938); M. A. Bender and M. A. Barcinski, *Cytogenetics* **8**, 251 (1969).
5. D. Scott, H. Sharpe, A. L. Batchelor, H. J. Evans, D. G. Papworth, *Mutat. Res.* **8**, 367 (1969).
6. A. L. Brooks, R. O. McClellan, S. A. Benjamin, *Radiat. Res.* **52**, 481 (1972).
7. A. L. Brooks, J. C. Retherford, R. O. McClellan, *ibid.* **59**, 693 (1974); L. R. McKay, A. L. Brooks, R. O. McClellan, *Health Phys.* **22**, 633 (1972).
8. A. L. Brooks, J. A. Mewhinney, R. O. McClellan, *Health Phys.* **22**, 701 (1972).
9. A. M. Kellerer and H. H. Rossi, *Radiat. Res.* **47**, 15 (1971).
10. W. C. Dewey, *Int. J. Radiat. Biol.* **22**, 95 (1972); ———, S. C. Furman, H. H. Miller, *Radiat. Res.* **43**, 561 (1970).
11. D. Scott, M. Fox, B. W. Fox, *Mutat. Res.* **22**, 207 (1974).
12. P. C. Koller, *The Role of Chromosomes in Cancer Biology*, P. C. Koller, Ed. (Springer-Verlag, New York, 1972), p. 6.
13. *The RBE for High-LET Radiations with Respect to Mutagenesis* (Pergamon, Oxford, 1972), p. 37.
14. Research performed under ERDA contract E(29-2)-1013 and conducted in facilities fully accredited by the American Association for Accreditation of Laboratory Animal Care.

23 May 1975; revised 25 August 1975

Albugo-Like Oogonia from the American Carboniferous

Abstract. *Fungal oogonia morphologically similar to those in the extant genus* Albugo *have been discovered in the integumental tissues of the fossil gymnosperm ovule* Nucellangium. *Disease symptoms in the fossil ovule are similar to those produced by* Albugo *in living angiosperm hosts.*

Fungal oogonia found in the integumental tissues of a Paleozoic ovule, *Nucellangium*, bear a striking resemblance to those of the extant Phycomycete (Oomycete) genus *Albugo*. Specimens are preserved in coal ball petrifications collected near Oskaloosa, Iowa, from middle Pennsylvanian strata. Of special significance is the fact that the oogonia are found in the so-called proliferated form of *Nucellangium* ovules (*1*). Proliferated ovules are slightly larger than normal ones and are characterized by irregular masses of parenchyma which extend into the locule of the ovule (Fig. 1a), giving the impression of an uncontrolled cancerous-type growth.

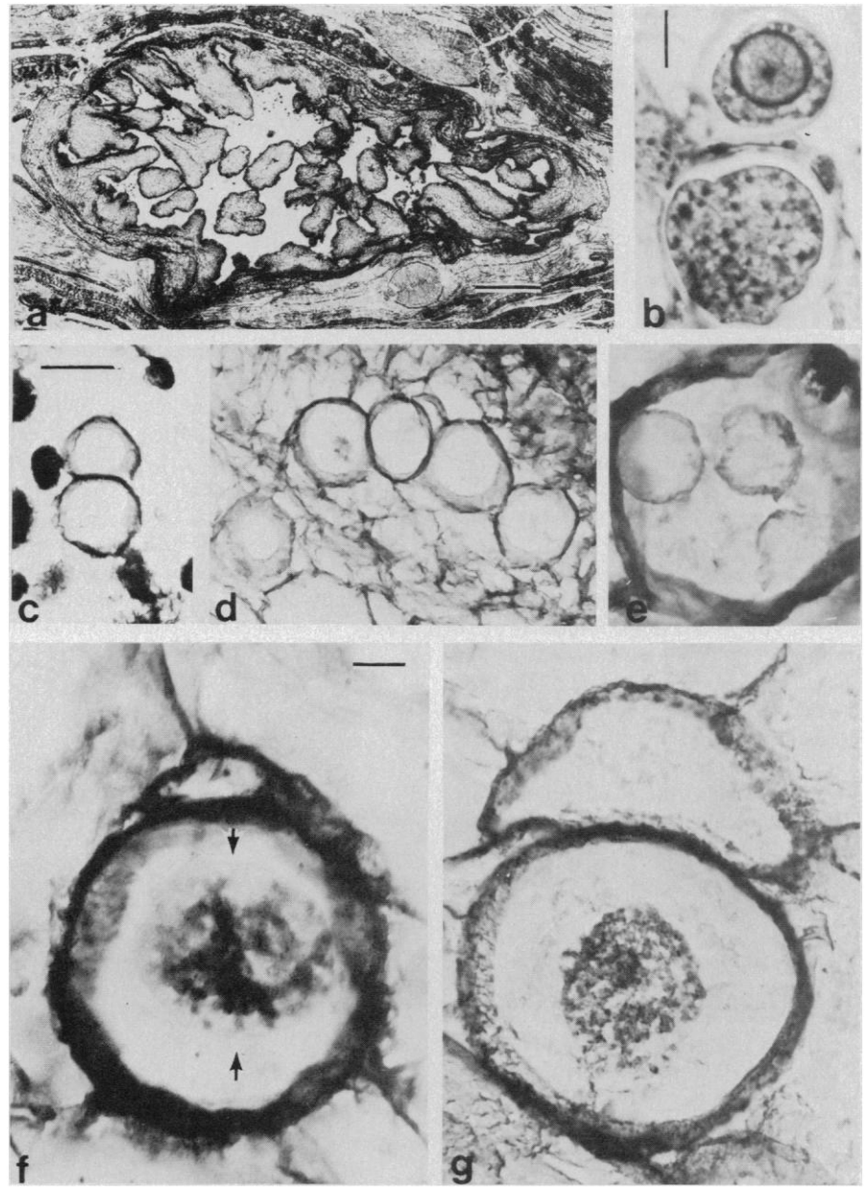

Fig. 1. (a) Section of proliferated ovule showing fingerlike extensions of integument into locule; scale bar, 2 mm. (b) Two *Albugo* oogonia, the top one containing oosphere within surrounding periplasm; scale bar, 20 μm. (c to g) Fossil oogonia. (c) Pair of oogonia free in locule of ovule; scale bar, 100 μm. (d) Oogonia in ovule integument; same scale as (c). (e) Oogonium with two visible spherical inclusions; same scale as (f). (f) Oogonium with membrane-bounded structure (arrows indicate membrane) interpreted as an oosphere; scale bar, 20 μm. (g) Oogonium with antheridium "hat cell" at top; same scale as (f).

Oogonia are not found in the parenchyma lobes; rather, they are consistently located around the periphery of the ovule, about 1 mm or less beneath the surface.

Albugo (Fig. 1b) is the infective agent responsible for white rust disease of crucifers. The symptoms are hypertrophy and hyperplasia, resulting in enlarged and distorted organs, particularly flower parts. These symptoms are the same as those exhibited in *Nucellangium*. The fossil oogonia not only are morphologically similar to *Albugo* but apparently produced the same symptoms in the host plant.

Fossil oogonia are spherical (90 to 100 μm in diameter) and usually have darker, thicker walls than the surrounding integumental parenchyma (Fig. 1d). Some have a dark central mass surrounded by a lighter, less dense zone (Fig. 1, f and g). These regions correspond to the egg (oosphere) and peripheral periplasm in *Albugo*. Some appear immature (before delimitation of the egg) and some older, having developed a reticulate structure on the surface of the maturing egg. None show a thick-walled oospore stage. Oogonia may be contiguous with one another or isolated among parenchyma cells (Fig. 1d). In some areas the integument of the ovule is disintegrated and oogonia are found free in the interior of the ovule or in the coal ball matrix outside the ovule. They sometimes occur in pairs (Fig. 1c). Two of the hundred or more oogonia in the ovule contain two to four spherical inclusions (oospheres?) (Fig. 1e).

Antheridium-like structures are in contact with some oogonia (Fig. 1g) but it is possible that these are only fortuitous juxtapositions of adjacent parenchyma cells or partial sections of adjacent oogonia. The largest such structure is shown in Fig. 1g; others are smaller. We have been unable to find fertilization tubes extending inward to the egg.

There are, of course, differences between the fossil and *Albugo* oogonia, one being the larger size of the fossil forms. Nevertheless, the close morphological similarity, together with the symptoms produced in the host plant organs, argues strongly for a close (congeneric) taxonomic relationship between the fossil and extant fungi. If so, this is the first report of *Albugo* from the fossil record.

Nucellangium is undoubtedly a gymnosperm ovule (we have evidence that it was borne on the Paleozoic gymnosperm *Cordaites*) and is now extinct. Extinction of the host necessitated the adaptation of the parasite to a new host group, a transition from a gymnosperm to angiosperms in this case. If our conclusion about the taxonomic affinity of the fossil oogonia (and the parent plant of *Nucellangium*) is correct, it should be possible to find other stages in the life cycle of the fungus on *Cordaites* leaves and stems.

B. M. STIDD
K. COSENTINO
Department of Biological Sciences, Western Illinois University, Macomb 61455

References and Notes

1. H. N. Andrews, *Ann. Mo. Bot. Gard.* **36**, 479 (1949).
2. We thank D. P. Rodgers and V. K. Howe for their comments on the identity of the fossil oogonia.

31 July 1975; revised 25 August 1975

High Speed Scintillation Autoradiography

Abstract. *Impregnation of nuclear track emulsion with liquid scintillator and exposure at –85°C allows rapid autoradiographic labeling. With tritiated thymidine of high specific activity (40 to 60 curies per millimole), exposure time can be shortened to 20 to 60 minutes, allowing complete sample processing within 4 hours. In experiments requiring isotopes with low incorporation rates or low specific activity, exposure time can be shortened from months to several days.*

The time required for standard autoradiography has limited many potential clinical and research applications of the technique. Although in vitro cell cycle analysis could provide useful information for planning chemotherapy for patients with acute leukemia (*1*) or for monitoring response to chemotherapy in patients with solid tumors (*2*), determination of the tritiated thymidine labeling index (percentage of cells going through scheduled DNA synthesis) with conventional autoradiography (ARG) requires at least 6 days to complete (*3*). For other applications in which uptake of tritiated thymidine is low or in which low specific activity is required, or both, ARG exposure times of 6 to 8 months are necessary.

Recent modifications of standard ARG have included the use of tritiated thymidine of higher specific activity (6 c/mmole), which gives results in 24 to 48 hours (*4*). A preliminary report (*5*) has also indicated that the use of a scintillator along with tritiated thymidine of low specific activity can also shorten the process. Using tritiated thymidine of high specific activity (40 to 60 c/mmole), a liquid scintillator, and a low temperature (–85°C) for emulsion exposure, we have developed techniques for very high speed scintillation autoradiography (HSARG). With these techniques, exposure times can be shortened to 20 minutes, and fresh blood, bone marrow, and tumor cell samples can be processed and stained to provide tritiated thymidine labeling results within 4 to 5 hours.

Heparinized cell suspensions (0.5×10^6 to 1.0×10^6 cells per milliliter) are incubated for 1 hour at 37°C with the high specific activity (40 to 60 c/mmole) tritiated thymidine (isotope dose, 5.0 μc per milliliter of cell suspension). (See discussion of effect of isotope dose, below.) Cytocentrifuge smears are then made on gelatin-coated slides and fixed with methanol. In the darkroom the slides are then dipped for 10 seconds into Kodak NTB_3 nuclear track emulsion at 42°C. After drying for 1 hour at room temperature (22°C), the slides are dipped for 10 seconds into the scintillator solution (22°C). The scintillator consists of 35 g of 2,5-diphenyloxazole (PPO) and 100 mg of 1,4-bis-2-(4-methyl-5-phenyloxazolyl)-benzene (dimethyl-POPOP) dissolved in 500 ml of dioxane. The scintillator-impregnated emulsion is exposed in the dark for 20 to 60 minutes at –85°C. (See discussion of temperature effect, below.) Slides are then developed at 17°C (*3, 6*). The cytocentrifuge smears are stained through the emulsion with Giemsa stain (*7*).

Multiple experiments were performed with normal, Hypaque-Ficoll-separated (*8*), phytohemagglutinin-stimulated human lymphocytes as a convenient source of cells with a high proportion undergoing rapid DNA synthesis. Five hundred cells were counted per slide, and experiments were done in duplicate or triplicate. Analysis of duplicate samples revealed that a twofold difference in labeling index (percentage) was statistically significant ($P < .05$).

The activation of silver crystals in the photographic emulsion used in autoradiography is dependent upon the number and energy of the beta emissions penetrating the emulsion. With standard ARG the level of beta emission is relatively low. However, with an isotope of very high specific activity (such as the tritiated thymidine used in our studies), there are many more beta emissions per molecule of incorporated isotope. When, in addition, the emulsion is impregnated with scintillator, photons are released as the electrons (beta particles) pass through the scintillator, and this activates even more silver crystals in the emulsion (Fig. 1). Increased sensitivity is accompanied by a slight increase in the scatter of emissions.